

An application of large displacement limit analysis to frame structures

Noël Challamel[†]

Laboratoire de Génie Civil et Génie Mécanique (LGCGM), INSA de Rennes, Université Européenne de Bretagne 20, avenue des Buttes de Coësmes, 35043 Rennes cedex, France

(Received July 18, 2007, Accepted July 20, 2009)

Abstract. The aim of this paper is to give a rigorous framework for the interpretation of limit analysis results including large displacements. The presentation is oriented towards unidimensional media (beams) but two-dimensional (plates) or three-dimensional media are also concerned. A single-degree-of-freedom system is first considered: it shows the basic phenomena of large displacement limit analysis or second-order limit analysis. The results are compared to those of a continuous system and the differences between both systems are discussed. Theoretical results are obtained using the kinematical approach of limit analysis. An admissible load-displacement plane is then defined, according to the yield design theory. The methodology used is applied to frame structures. The presented results are nevertheless different from those already published in the literature, as the virtual displacement field can be distinguished from the displacement field at collapse. The simplicity of large displacement limit analysis makes it attractive for practical engineering applications. The load-displacement upper bound can be used for instance in the optimal design of steel frames in seismic areas.

Keywords: limit analysis; stability; kinematics; frames; seismic design; geometric nonlinearity; plasticity; geometrically exact analysis; large displacement.

1. Introduction

Results of limit analysis are conventionally obtained assuming both that the material is perfectly plastic and that the geometrical change can be neglected (Salençon 2002 for instance). The first assumption can be questionable for structural elements in the hardening range or in the softening range (see for instance Jirasek and Bazant 2002). The second assumption is related to geometrical changes. Effects of geometrical change can be predominant for elastoplastic structures (Horne and Merchant 1965, Horne 1995, Yu and Zhang 1996, Bazant and Cedolin 2003, Shanmugan and Wang 2005 or Chakrabarty 2007). These effects can increase or decrease the strength capacity of the equivalent structure analysed without any geometrical changes. Civil engineers have to quantify these effects, using numerical simulations or simplified analytical methods, especially in earthquake engineering design when large displacements analysis, are often necessary (Jennings and Husid 1968, or more recently Yang *et al.* 2003). Only geometrical change effects are treated in this paper.

[†] E-mail: Noel.Challamel@insa-rennes.fr

The aim of this paper is to give a rigorous framework for the interpretation of existing limit analysis results including large displacements. It is motivated by the apparent efficiency of these analytical methods in comparison with numerical simulations of the evolution problem, but also by the simplicity of such approaches that are commonly used for practical applications.

It seems that the first studies dealing with large displacement limit analysis were applied to beam structures. Merchant (1954) first suggested intuitive ideas that stability may affect the load carrying capacity of frames. These results were included in a more general limit analysis framework including large displacements (Onat 1955, Massonnet and Save 1961, Horne 1963, Horne 1995, Save *et al.* 1997). The analytical method is based on the kinematic approach, using only rigid plastic virtual mechanism. The interpretation of these results is discussed later in the paper. To our knowledge, no results have been found concerning the static approach. These analytical methods are completed nowadays by numerical simulations generally based on second-order analysis (Liew *et al.* 1993, Elnashai 2001, Leu and Tsou 2001, Chiou *et al.* 2002 - see more recently Chan and Zhou 2004 or Zhou and Chan 2004).

The kinematic approaches of large displacement limit analysis are also used for two dimensional structures such as plates (see for instance Calladine 1968). It is also the case of the works of Climenhaga and Johnson (1972), who studied the post-yield behaviour of I-steel beams with an out-of-plane kinematic approach. These kinematical approaches may be extended nowadays to other mechanisms of steel structural members (see for instance Mazzolani and Gioncu 2002). Let us denote that three-dimensional problems can also exhibit strong large displacements effects. The usual example is the elastoplastic expansion of a spherical cavity in an infinite media, which was treated in detail by Salençon (1966). Despite numerous theoretical investigations into the stability, existence or uniqueness of the elastoplastic evolution problem in presence of large displacements (Lance and Soechting 1970, Gürkök and Hopkins 1973, Maier and Drucker 1973, Duszek and Lodygowski 1983, de Freitas and Smith 1984 or Weichert 1990, Polizzotto and Borino 1996), it seems that very few theoretical results of limit analysis are available for practical applications.

This paper is devoted to limit analysis including large displacements. A single-degree-of-freedom system is first considered. The simple analytical model can be solved completely with closed-form solutions: it shows the basic phenomena of large displacement limit analysis. The results are compared with those of a continuous system and the differences between both systems are discussed. Theoretical results are obtained using the kinematical approach of limit analysis. An admissible load-displacement plane is then defined, according to the theory of yield design (Challamel 2006). The methodology is applied to frame structures and the frame example treated by Onat (1955) or Massonnet and Save (1961) is commented.

2. Single-degree-of-freedom system

The simple single-degree-of-freedom system of Fig. 1 is considered. The elastoplastic law is elastic and perfectly plastic, as part of the fundamental assumption of limit analysis. A rigid bar is solicited by a vertical force P and a horizontal force H (Fig. 1). This bar is connected to an elastic spring of stiffness k at the base (in the elastic phase). The length of the bar is equal to L . This is a single-degree-of-freedom system, whose variable is the rotation denoted by θ . The horizontal displacement u of the top of the column can be expressed in terms of this degree-of-freedom

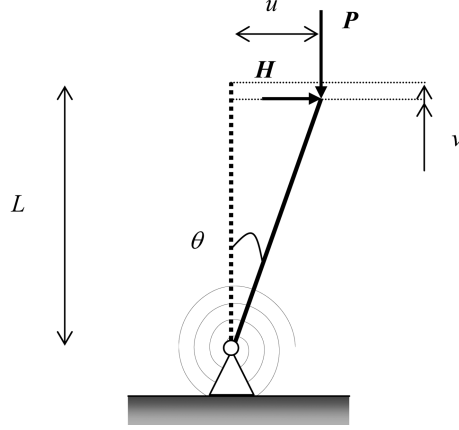


Fig. 1 Single-degree-of-freedom-system

$$u = L \sin \theta \quad (1)$$

The study deals with the monotonic response of the horizontal force H versus the horizontal displacement u for fixed value of vertical force P . The vertical displacement v is given by

$$v = L(1 - \cos \theta) \quad (2)$$

In the elastic phase, the internal energy of this system is equal to

$$E(\theta) = \frac{1}{2}k\theta^2 - HL\sin\theta - PL(1 - \cos\theta) \quad (3)$$

Equilibrium positions are calculated from the stationary condition $dE/d\theta = 0$, which brings us to the following equation

$$\frac{H(\theta)}{P_{cr}} = \frac{\theta}{\cos\theta} - \eta \cdot \tan\theta \quad \text{with} \quad \left\{ \begin{array}{l} P_{cr} = \frac{k}{L} \\ \eta = \frac{P}{P_{cr}} \in [0;1] \end{array} \right. \quad (4)$$

P_{cr} is the critical load of the system with $H = 0$. For sufficiently small values of θ , Eq. (4) can also be expressed by the linear approximation

$$\frac{H(\theta)}{P_{cr}} = (1 - \eta)\theta \quad \text{or} \quad H(u) = (1 - \eta)\frac{k}{L^2}u \quad (5)$$

The vertical load acts as it reduces linearly the stiffness of the system without vertical force (commonly called the “ P - Δ ” effect). η is a dimensionless coefficient and is sometimes called the stability coefficient (Bernal 1987).

The relation given by Eq. (4) is plotted in Fig. 2 for various values of η . H has been expressed in terms of the horizontal displacement u , from Eq. (1). H is a non-linear function of the displacement, in the so-called exact geometry. Previous equations are valid in the elastic phase where the moment

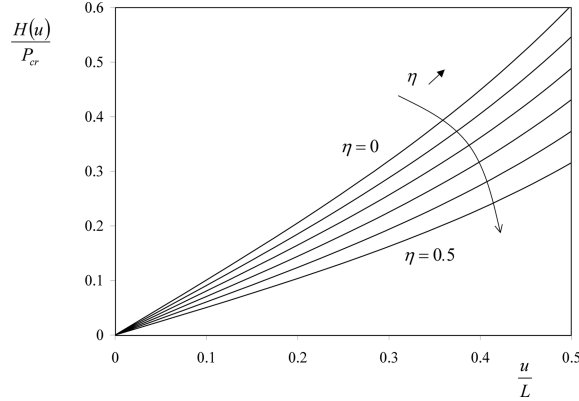


Fig. 2 Lateral load versus lateral displacement for various level of vertical load – elastic case

M remains in the elastic domain. The spring has in fact a perfect elastoplastic behaviour, with a yield moment, usually denoted by M_p . The load criterion can be given by

$$f(M) = |M| - M_p \leq 0 \quad (6)$$

The characteristic rotation may be introduced from the plastic moment and the elastic stiffness ($\theta_y = M_p/k = u_y/L$). In the case of monotonic loading, equilibrium equations directly give

$$M_p = H(L - v) + Pu \quad (7)$$

For θ greater than θ_y , the plastic evolution gives rise to the new function $H(\theta)$

$$\frac{H(\theta)}{P_{cr}} = \frac{\theta_y}{\cos \theta} - \eta \cdot \tan \theta \text{ and } \theta = \arcsin\left(\frac{u}{u_y} \theta_y\right) \quad (8)$$

For sufficiently small values of θ (second order analysis), Eq. (8) may be approximated by

$$\frac{H(\theta)}{P_{cr}} = \theta_y - \eta \cdot \theta \Rightarrow \frac{H(u)}{\frac{M_p}{L}} = 1 - \eta \frac{u}{u_y} \quad (9)$$

The relation given by Eq. (8) is plotted in Fig. 3 for various values of θ_y at constant value $\eta = 0.25$. Results obtained from an exact geometrical analysis are presented for various yield rotation values (Fig. 3). It is recognised that large values of θ_y are irrelevant for practical applications, but it is necessary to employ such large values in order to illustrate any effect of large displacement theory. It appears that the response is almost linear in the loading phase: second order analysis is a good approximation in the elastic phase. This result is found again in the post-yield regime for small and realistic yield rotation values. The influence of the type of geometrical analysis is plotted in Fig. 4. Second order analysis affects both the stiffness and the post-yield regime (Fig. 4). This analysis is very close to the exact geometry analysis with these parameters. The maximum lateral force between standard limit analysis and large displacement limit analysis can be significant. Using Eq. (5) obtained from the second order analysis, the ratio between maximum lateral forces in both analysis (large displacement analysis and standard limit analysis) is equal to $1 - \eta$. In some other

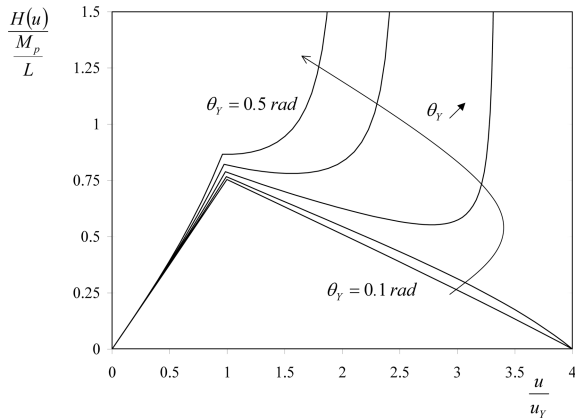


Fig. 3 Lateral load versus lateral displacement for various level of vertical load – elastoplastic case; $\eta = 0.25$

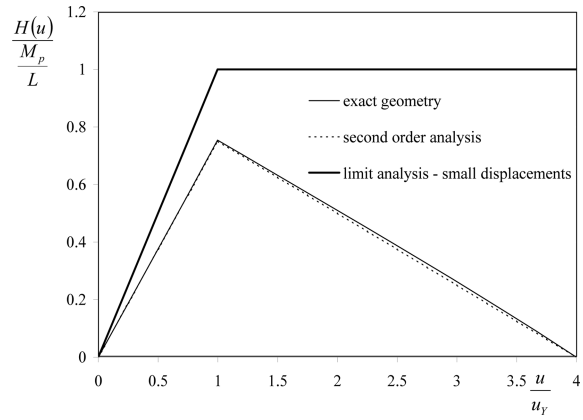


Fig. 4 Lateral load versus lateral displacement – influence of the geometrical analysis; $\eta = 0.25$; $\theta_\gamma = 0.1$ rad

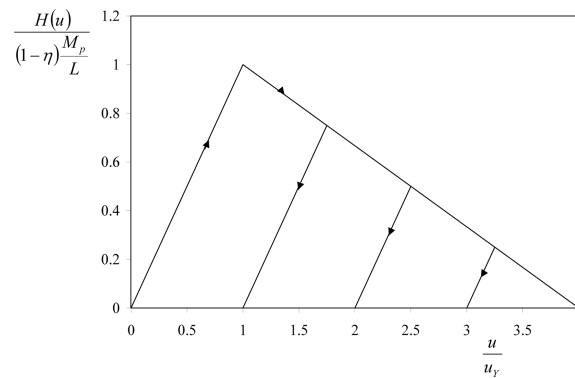


Fig. 5 Non-linear geometrical effects as a global elastoplastic softening spring; $\eta = 0.25$

cases, standard limit analysis can give smaller maximum forces than large displacement limit analysis (Fig. 3).

Fig. 5 shows the global force-displacement response including unloading range. It can be concluded that geometrical non-linearity can also be described within an elastoplastic softening spring, whose softening is linear when the second order assumption is considered. As a conclusion, geometrical non-linearity can be treated in the same way as simple material non-linearity (see also Challamel and Pijaudier-Cabot 2006).

3. Principle of limit analysis in large displacements

The virtual work principle expresses the equilibrium requirement in its dual form

$$\delta W_{int} = \delta W_{ext} \tag{10}$$

where δW_{int} is the work of the internal force associated with the virtual motion and δW_{ext} is the work of the external force. For the single-degree-of-freedom system of Fig. 1, this relation reduces to

$$M\delta\theta = H\delta u + P\delta v \quad (11)$$

From Eq. (1) and Eq. (2), the relation between the rotation and the displacements is obtained from

$$\begin{cases} \delta u = L\cos\theta\delta\theta \\ \delta v = L\sin\theta\delta\theta \end{cases} \quad (12)$$

The kinematic approach will lead to the determination of an upper bound estimate of the lateral force. Using Eq. (6), the work of the internal force is surrounded by

$$M\delta\theta \leq M_p|\delta\theta| \quad (13)$$

Eqs. (11), (12) and (13) lead to the following inequality

$$HL\cos\theta\delta\theta + PL\sin\theta\delta\theta \leq M_p|\delta\theta| \quad (14)$$

Such upper bound results in the two following inequalities

$$\frac{-M_p - PL\sin\theta}{L\cos\theta} \leq H \leq \frac{M_p - PL\sin\theta}{L\cos\theta} \quad (15)$$

This equation can be written using the displacement variables

$$\frac{-M_p - Pu}{L - v} \leq H \leq \frac{M_p - Pu}{L - v} \quad (16)$$

For this single-degree-of-freedom system, v is expressed as a function of u

$$\frac{v}{L} = 1 - \cos\left(\arcsin\left(\frac{u}{L}\right)\right) \quad (17)$$

Eq. (16) can be simplified using second order analysis assumptions ($v \ll L$)

$$\frac{-M_p - Pu}{L} \leq H \leq \frac{M_p - Pu}{L} \quad (18)$$

Let us remark that this approximation is not within levels of safety. Inequalities (18) can be rewritten as

$$-1 - \eta \frac{u}{u_Y} \leq \frac{H(u)}{\frac{M_p}{L}} \leq 1 - \eta \frac{u}{u_Y} \quad (19)$$

It can be checked that Eq. (7) comply with the bounds of Eq. (16). For this problem, the upper bound is reached during the elastoplastic evolution problem. This method shows that the upper bound is now defined in a (H, u) plane (force-displacement diagram), which is of course not the case of standard limit analysis. The boundary of the admissible (H, u) evolution (in the sense of yield design theory) can be a non-linear boundary, in the case of large displacements assumption. Fig. 6 illustrates the graphical upper bound, obtained from the second-order analysis, using inequalities of Eq. (18).

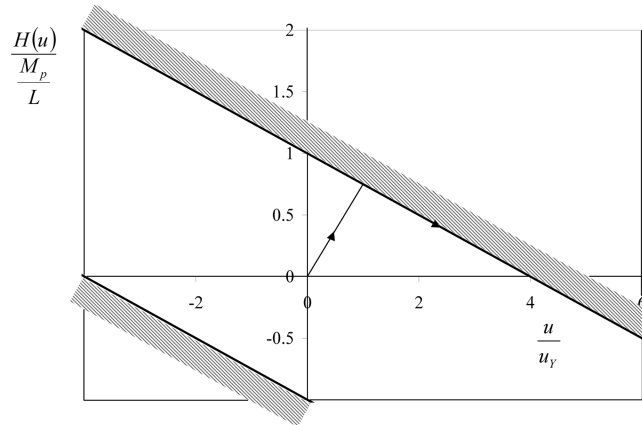


Fig. 6 Kinematical approach applied to large displacement limit analysis; $\eta = 0.25$

The result Eq. (16) can be found again using the static approach from outside (see Salençon 1990 for the meaning of this approach and the link between kinematical approach by outside)

$$|M| \leq M_p \Rightarrow |Pu + H(L - v)| \leq M_p \quad (20)$$

The inequality Eq. (20) leads to the same result of Eq. (16).

4. Two-degrees-of-freedom system

A two-degrees-of-freedom system (θ_1, θ_2) is now considered (see Fig. 7). One recognizes the academic Ziegler's model (Ziegler 1968), often investigated in non-conservative elastic systems. However, in the present case, the loading is conservative but the connection are elastically and perfectly plastic (with stiffness k , and plastic moment M_p). For this structural system, the direct

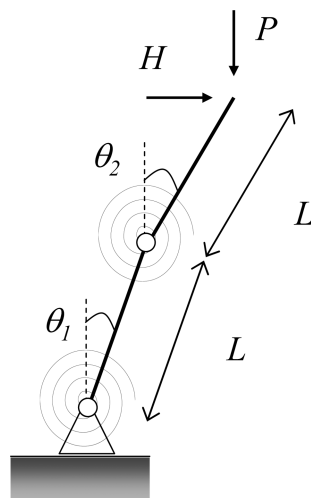


Fig. 7 Two-degrees-of-freedom system

application of large displacement limit analysis would be based on the virtual rotation field

$$\delta\theta_1 = \delta\theta_2 = \delta\theta_0 \quad (21)$$

The upper bound function is then deduced, in the so-called geometrically exact framework

$$\delta W_{ext} \leq M_p |\delta\theta_0| \Rightarrow HL(\cos\theta_1 + \cos\theta_2) + PL(\sin\theta_1 + \sin\theta_2) \leq M_p \quad (22)$$

This upper bound can be simplified in the second-order analysis

$$H \leq \frac{M_p}{2L} - \frac{P}{2}(\theta_1 + \theta_2) \quad (23)$$

It can be shown that this bound is exactly reached during the evolution problem assuming the second-order analysis, and the mode of collapse is then described by

$$H = \frac{M_p}{2L} - \frac{P}{2}(\theta_1 + \theta_2) \quad (24)$$

Moreover, the following inequalities can be obtained at collapse

$$\theta_1 < \theta_2 \Rightarrow \frac{M_p}{2L} - P\theta_2 < \frac{M_p}{2L} - \frac{P}{2}(\theta_1 + \theta_2) < \frac{M_p}{2L} - P\theta_1 \quad (25)$$

It is worth mentioning that most reasoning published in the literature, on large displacement limit analysis, are based on the coexistence of the virtual and the true collapse rotation field. In this case, this assumption would lead to the un-correct result

$$\theta_1 = \theta_2 = \theta_0 \Rightarrow H \leq \frac{M_p}{2L} - P\theta_0 \Rightarrow H \leq \frac{M_p}{2L} - P\theta_2 \quad (26)$$

It can be seen from Eq. (25), that the last inequality of Eq. (26) is in contradiction with Eq. (24).

5. Continuous system - Differential equations

The same methodology can be applied to multi-degrees-of-freedom systems or continuous systems (Fig. 8). The continuous system of Fig. 8 can be viewed as a generalisation of the single-degree-of-freedom system of Fig. 1, or the two-degrees-of-freedom system of Fig. 7. The rod is assumed to be inextensible. This case has been already treated for the elastic phase by Ziegler (1968). The rod is loaded by a vertical force P and a horizontal force H at the upper point. L is the length of the rod. The homogeneous rod is composed of an elastoplastic perfect material, whose elastic flexural rigidity is denoted by EI , and the yield moment is denoted by M_p . The column is built in at the basis. The rotation is the unknown function of the curvilign coordinate $s \rightarrow \theta(s); s \in [0; L]$. The origin ($s = 0$) is chosen at the basis of the column. The deflection is denoted by $\omega(s)$. The virtual work principle expresses the equilibrium requirement in its dual form

$$\int_0^L M \delta\chi ds = H \delta u + P \delta v \quad \text{with} \quad \begin{cases} u = \int_0^L \sin\theta(s) ds \\ v = L - \int_0^L \cos\theta(s) ds \end{cases} \quad (27)$$

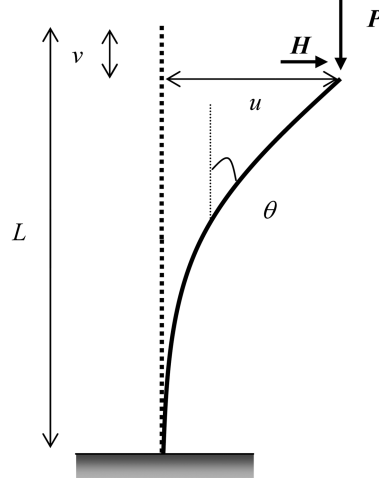


Fig. 8 Continuous system

M is the bending moment and χ is the curvature. The elastic behaviour is first studied

$$\int_0^L EI \theta'(s) \delta \theta'(s) ds = H \int_0^L \cos \theta(s) \delta \theta(s) ds + P \int_0^L \sin \theta(s) \delta \theta(s) ds \quad (28)$$

By integrating the first term by parts and using the boundary conditions, the non linear differential equation follows

$$EI \theta''(s) + H \cos \theta(s) + P \sin \theta(s) = 0 \quad (29)$$

The *Elastica* problem of Euler (1744) is recognised when only a vertical force is applied. Solutions of Eq. (29) can be investigated using elliptic functions (Antman 1995). It is worth mentioning at this stage that the *Plastica* problem (with an elastic perfectly plastic stress-strain law) was investigated by Yu and Johnson (1982) (see also Yu and Zhang 1996). The same problem with an inclined concentrated force was considered by Feng and Tong-Xi (1991). Numerical results of the large deflection of an elastoplastic cantilever have been provided by Wang *et al.* (1995).

The second-order analysis leads to the much simpler linear differential equation

$$EI \theta''(s) + P \theta(s) = -H \quad (30)$$

The dimensionless loading parameters can be introduced as

$$\left| \begin{array}{l} \eta = \frac{P}{P_{cr}} \\ h^* = \frac{H}{P_{cr}} \end{array} \right. \quad \text{with} \quad P_{cr} = \frac{\pi^2 EI}{4L^2} \quad (31)$$

As in the first part, P_{cr} is the critical load of the system with $H = 0$. The solution of the differential Eq. (30) is written as

$$\theta(s) = A \cos \frac{\pi \sqrt{\eta}}{2L} .s + B \sin \frac{\pi \sqrt{\eta}}{2L} .s - \frac{h^*}{\eta} \quad (32)$$

Constants A and B are determined using the boundary conditions $\theta(0) = 0$ and $\theta'(L) = 0$. Finally, the solution can be written as

$$\theta(s) = \frac{h^*}{\eta} \cos \frac{\pi\sqrt{\eta}}{2L} \cdot s + \frac{h^*}{\eta} \tan \frac{\pi\sqrt{\eta}}{2} \sin \frac{\pi\sqrt{\eta}}{2L} \cdot s - \frac{h^*}{\eta} \quad (33)$$

and consequently

$$w(s) = \frac{2Lh^*}{\pi\eta\sqrt{\eta}} \sin \frac{\pi\sqrt{\eta}}{2L} \cdot s - \frac{2Lh^*}{\pi\eta\sqrt{\eta}} \tan \frac{\pi\sqrt{\eta}}{2} \cos \frac{\pi\sqrt{\eta}}{2L} \cdot s - \frac{h^*}{\eta} s + \frac{2Lh^*}{\pi\eta\sqrt{\eta}} \tan \frac{\pi\sqrt{\eta}}{2} \quad (34)$$

The displacement u is obtained from

$$u = w(L) = \frac{2Lh^*}{\pi\eta\sqrt{\eta}} \left(\tan \frac{\pi\sqrt{\eta}}{2} - \frac{\pi\sqrt{\eta}}{2} \right) \quad (35)$$

This displacement is infinite for $\eta = 1$, that is when the load P is equal to the critical load P_{cr} (the value of the critical load is confirmed by such a singularity). In the elastic phase, the relation between the horizontal force and the vertical force is therefore given by

$$\frac{H(u)}{P_{cr}} = \frac{\pi\eta\sqrt{\eta}}{2} \frac{1}{\tan \frac{\pi\sqrt{\eta}}{2} - \frac{\pi\sqrt{\eta}}{2}} \frac{u}{L} \quad (36)$$

It is not difficult to notice that

$$\max_{s \in [0;L]} |M(s)| = |M(0)| \quad (37)$$

It is sufficient to calculate

$$M'(s) = EI\theta''(s) = -H - P\theta(s) \leq 0 \quad (38)$$

M is a decreasing function of the s abscissa.

In the elastoplastic phase, the differential Eq. (30) is still valid and the new boundary conditions are

$$\begin{cases} \theta'(0) = \frac{M_p}{EI} \\ \theta'(L) = 0 \end{cases} \quad (39)$$

Integration gives the displacement at the yield point

$$w(s) = \frac{M_p}{P} \frac{1}{\tan \frac{\pi\sqrt{\eta}}{2}} \sin \frac{\pi\sqrt{\eta}}{2L} \cdot s - \frac{M_p}{P} \cos \frac{\pi\sqrt{\eta}}{2L} \cdot s - \frac{h^*}{\eta} s + \frac{M_p}{P} \quad (40)$$

In this case, it is easy to verify from Eq. (40) that

$$u = w(L) = \frac{-HL + M_p}{P} \quad (41)$$

Moreover, Eq. (38) shows that the bending moment M also decreases with s . The plastic hinge located at the basis will remain stationary within the second order analysis. Eq. (7) obtained in case

of large displacements assumption, is still valid

$$H = \frac{M_p - Pu}{L - v} \quad (42)$$

Assuming the second order analysis ($\theta(s) \ll 1 \Rightarrow v/L \ll 1$), the governing equation during the monotone elastoplastic evolution is obtained from

$$\frac{H}{M_p} = 1 - \frac{P}{M_p} \frac{u}{L} \quad (43)$$

Eq. (41) is found again. The evolution of the force-displacement diagram is very similar to that of Fig. 5.

6. Application of Large Displacement limit analysis - continuous system

The principle of kinematic approach of limit analysis is based on the virtual work principle

$$\int_0^L M \delta \chi ds + \sum_i M [\delta \theta]_i = H \delta u + P \delta v \quad (44)$$

where $[\delta \theta]$ denotes the jump of any quantity $\delta \theta$ at the point of abscissa s_i . The fundamental reasoning of yield design is based on the surrounding of the internal work with respect to the strength capacity of the rod (Salençon 2002)

$$H \delta u + P \delta v \leq \int_0^L M_p [\delta \chi] ds + \sum_i M_p [\delta \theta]_i \quad (45)$$

This inequality applied to the present case gives

$$H \int_0^L \cos \theta(s) \delta \theta(s) ds + P \int_0^L \sin \theta(s) \delta \theta(s) ds \leq \int_0^L M_p [\delta \chi] ds + \sum_i M_p [\delta \theta]_i \quad (46)$$

The most simple virtual displacement field is the rigid mechanism defined by

$$\delta \theta(s) = \delta \theta_0 \quad (47)$$

The inequality Eq. (46) is then reduced to

$$H \delta \theta_0 \int_0^L \cos \theta(s) ds + P \delta \theta_0 \int_0^L \sin \theta(s) ds \leq M_p |\delta \theta_0| \quad (48)$$

that can be written as

$$-M_p \leq H(L - v) + Pu \leq M_p \quad (49)$$

This is the same inequality as in Eq. (16) for the single-degree-of-freedom system. In this case however, the top displacement v is a function of $\theta(s)$ within the large displacement assumption. Assuming second order analysis, the inequality Eq. (18) is found again. Fig. 6 is still valid for the continuous rod. This result could be found again using the static approach by outside, previously

described: the moment is maximum at the basis (Eq. (37)). Eq. (20) is then necessarily valid, even if the moment function $M(s)$ has not been explicitly calculated. Equalities Eq. (42) or Eq. (43) show that the upper bound of the force-displacement diagram is effectively reached during elastoplastic evolution.

7. Application to frames – First example

The problem of the frame solved by Onat (1955) or Massonnet and Save (1961) is described in Fig. 9. Each element is assumed to be inextensible with a yield moment M_p . h is the height of the columns. The horizontal displacement u and the vertical displacement v can be expressed in terms of the rotation $\theta(s)$ in the loaded column

$$\begin{cases} u = \int_0^h \sin \theta(s) ds \\ v = h - \int_0^h \cos \theta(s) ds \end{cases} \quad (50)$$

The virtual displacement field considered in the kinematic approach is the rigid mechanism defined by

$$\delta\theta(s) = \delta\theta_0 \text{ in the columns; } \delta\theta(s) = 0 \text{ in the horizontal beam} \quad (51)$$

Inequality Eq. (45) is now expressed by

$$H\delta u + P\delta v \leq 2M_p|\delta\theta_0| \quad (52)$$

Using Eq. (50), the following inequalities appear

$$-2M_p \leq H(h-v) + Pu \leq 2M_p \quad (53)$$

The second order analysis gives the new simplified surrounding

$$-\frac{2M_p}{h} - P\frac{u}{h} \leq H \leq \frac{2M_p}{h} - P\frac{u}{h} \quad (54)$$

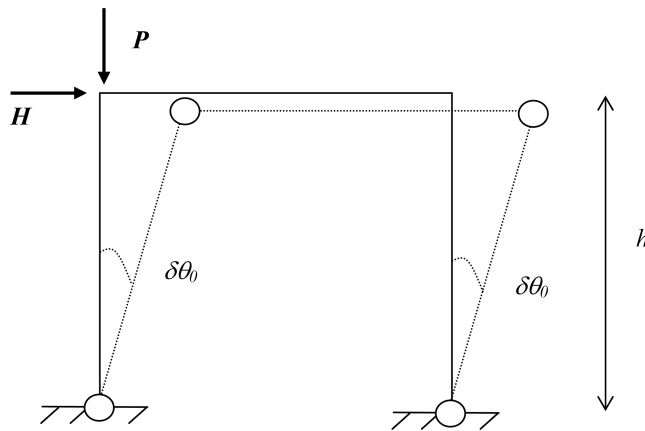


Fig. 9 Frame loaded by a vertical and a horizontal force – mechanism A

The terms appearing in Eq. (54) do not depend on the length of the horizontal beam. This reasoning is different from the standard one available in the literature, who expresses the virtual displacements by the equations

$$\begin{cases} \delta u = (h - v(\theta_0))\delta\theta_0 \\ \delta v = u(\theta_0)\delta\theta_0 \end{cases} \neq \begin{cases} \delta u = (h - v[\theta])\delta\theta_0 \\ \delta v = u[\theta]\delta\theta_0 \end{cases} \quad (55)$$

For the standard approach available in the literature (left terms of Eq. (55)), the displacements are postulated as a function of the virtual rotations (Onat 1955, Massonnet and Save 1961, Horne 1963, Horne 1995, Save *et al.* 1997). In the second case (the right terms of Eq. (55)), following the reasoning of the present paper, the displacements are expressed as functional of the unknown $\theta(s)$ function.

8. Application to frames – Second example

The frame considered in this part is described in Fig. 10. It is a generalisation of the previous one. The length of the beam is denoted by L . The force P is applied at a distance λL of the loaded column in the horizontal beam. The origin is taken at the basis of the loaded column. The horizontal displacement u and the vertical displacement v of the top of the loaded column can be expressed in terms of the rotation $\theta(s)$ in the loaded column

$$\begin{cases} u = \int_0^h \sin \theta(s) ds \\ v = h - \int_0^h \cos \theta(s) ds \end{cases} \quad (56)$$

The vertical displacement of the point loaded by the vertical force is equal to

$$v_p = v + \int_h^{h+\lambda L} \sin \theta(s) ds \quad (57)$$

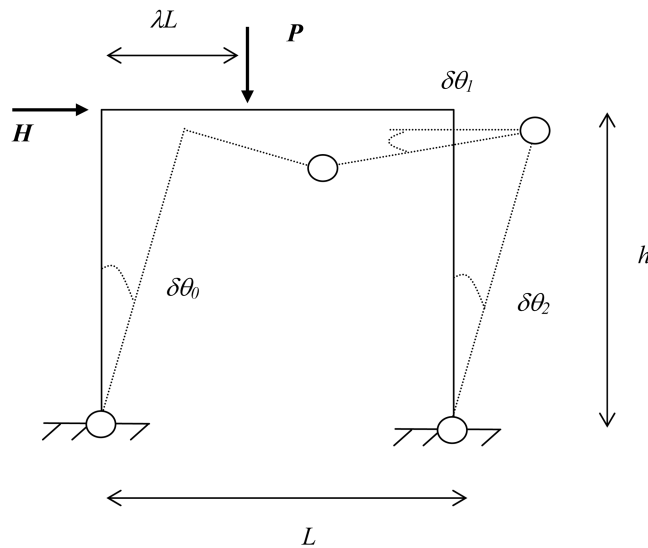


Fig. 10 Frame loaded by a vertical and a horizontal force – mechanism B

The external work contribution is equal to

$$\delta W_{ext} = H\delta u + P\delta v_p = H \int_0^h \cos \theta(s) \delta \theta(s) ds + P \int_0^h \sin \theta(s) \delta \theta(s) ds + P \int_h^{h+\lambda L} \cos \theta(s) \delta \theta(s) ds \quad (58)$$

As in Eq. (51), the simple mechanism described in Fig. 9, denoted mechanism *A*, is characterised by

$$\begin{cases} \delta \theta(s) = \delta \theta_0 & \text{for } s \in [0; h] \\ \delta \theta(s) = 0 & \text{for } s \in [h; L+h] \\ \delta \theta(s) = \delta \theta_0 & \text{for } s \in [L+h; L+2h] \end{cases} \quad (59)$$

Applying the kinematic approach of limit analysis, Eq. (45) is expressed in the same way by

$$-2M_p \leq H(h-v) + Pu \leq 2M_p \quad (60)$$

The second order analysis assumption reduces these inequalities in Eq. (54), that is still valid. The mechanism of Fig. 10, denoted by mechanism *B*, can also be used in the kinematic approach of limit analysis. It is defined by

$$\begin{cases} \delta \theta(s) = \delta \theta_0 & \text{for } s \in [0; h] \\ \delta \theta(s) = \delta \theta_0 & \text{for } s \in [h; h+\lambda L]; \delta \theta(s) = -\delta \theta_1 & \text{for } s \in [h+\lambda L; L+h] \\ \delta \theta(s) = \delta \theta_2 & \text{for } s \in [L+h; L+2h] \end{cases} \quad (61)$$

The general study of articulated mechanism with four hinges was first studied by Grashoff during the nineteenth century. Without any assumptions on the size of virtual rotations, the non-linear system of unknown $(\delta \theta_0, \delta \theta_1, \delta \theta_2)$ is as follows (Arakélian 1997)

$$\begin{cases} \sqrt{\alpha^2 + \lambda^2} \sin(\varphi + \delta \theta_0) + (1-\lambda) \cos(\delta \theta_1) - \alpha \sin(\delta \theta_2) = 1 \\ \sqrt{\alpha^2 + \lambda^2} \cos(\varphi + \delta \theta_0) + (1-\lambda) \sin(\delta \theta_1) - \alpha \cos(\delta \theta_2) = 0 \end{cases} \quad \text{with} \quad \begin{cases} \alpha = \frac{h}{L} \\ \tan \varphi = \frac{\lambda}{\alpha} \end{cases} \quad (62)$$

Closed-form solutions of this system are available. As a consequence, the top of the first column is generally not at the same height as the top of the second column. The kinematic approach of limit analysis is applied using the virtual displacement field of Eq. (61)

$$\delta \theta_0 H(h-v) + \delta \theta_0 P u + \delta \theta_0 P \int_h^{h+\lambda L} \cos \theta(s) ds \leq M_p |\delta \theta_0 + \delta \theta_1| + M_p |\delta \theta_1 + \delta \theta_2| \quad (63)$$

Eq. (63) is a complex functional inequality of the displacement function. Second order analysis is used assuming that both the true and the virtual rotations are small

$$\theta(s) \ll 1 \quad \text{and} \quad \delta \theta(s) \ll 1 \quad (64)$$

In this case, the strong non-linear system Eq. (62) is converted into a linear one

$$\begin{cases} \delta \theta_1 = \frac{\lambda}{1-\lambda} \delta \theta_0 & \text{and } \lambda \in]0; 1[\\ \delta \theta_2 = \delta \theta_0 \end{cases} \quad (65)$$

The new relation does not depend on the size of the columns. Eq. (63) is now expressed by

$$\delta\theta_0 H h + \delta\theta_0 P(u + \lambda L) \leq \frac{2}{1-\lambda} M_p |\delta\theta_0| \quad (66)$$

For $\delta\theta_0 \geq 0$, Eq. (54) and Eq. (66) can be summarised in

$$\left. \begin{array}{l} \text{mechanism A: } \frac{H}{\frac{2M_p}{h}} \leq 1 - \frac{1}{\lambda(1-\lambda)} \frac{P u}{P^+ L} \\ \text{mechanism B: } \frac{H}{\frac{2M_p}{h}} \leq \frac{1}{1-\lambda} \left(1 - \frac{P}{P^+}\right) - \frac{1}{\lambda(1-\lambda)} \frac{P u}{P^+ L} \end{array} \right\} \text{with } P^+ = \frac{2M_p}{L\lambda(1-\lambda)} \quad (67)$$

P^+ is the first-order limit load of the frame without any lateral force H . The comparison between the upper bound obtained with each mechanism depends on the P/P^+ ratio.

$$\left. \begin{array}{l} \frac{P}{P^+} \in [0; \lambda]: \frac{H}{\frac{2M_p}{h}} \leq 1 - \frac{1}{\lambda(1-\lambda)} \frac{P u}{P^+ L} \\ \frac{P}{P^+} \in [\lambda; 1]: \frac{H}{\frac{2M_p}{h}} \leq \frac{1}{1-\lambda} \left(1 - \frac{P}{P^+}\right) - \frac{1}{\lambda(1-\lambda)} \frac{P u}{P^+ L} \end{array} \right\} \quad (68)$$

In the first case, mechanism *A* gives the best upper bound. In the second case, the best upper bound is obtained with mechanism *B*. The parameters chosen for the representation of Fig. 11 belong to this second case. The slope of the force-displacement upper bound is the same in both cases. For the case studied, P is applied at the middle of the beam ($\lambda = 0.5$). The vertical load is chosen as $P = 0.75P^+$.

Finally, the exact meaning of Fig. 11 can be commented in the following way: inequalities Eq. (68) are necessary conditions on the static and kinematic variables (P, H, u), that verify equilibrium equations and strength criterion (assuming a second-order analysis). This means that the

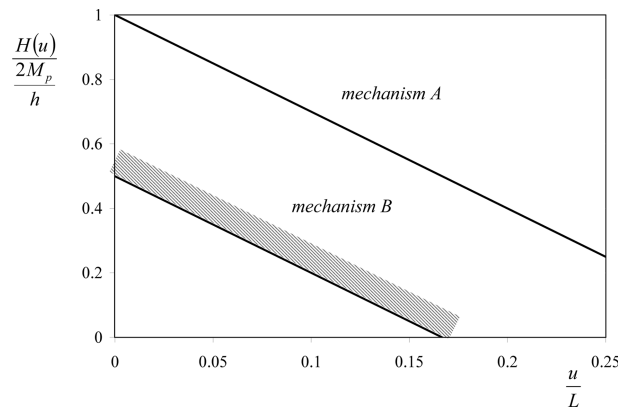


Fig. 11 Admissible force-displacement diagram – frame of Fig. 9; $P/P^+ = 0.75$; $\lambda = 0.5$

violation of inequalities Eq. (68) cannot ensure both equilibrium and strength criterion. Of course, generally, inequalities Eq. (68) are not sufficient conditions of equilibrium and strength, as in the standard kinematic approach of yield design (Salençon 1990, Salençon 2002).

9. Application to frames – Third example

A third example of a multi-storey single-bay portal is now studied (see Fig. 12). The horizontal displacement u and the vertical displacement v of the loaded point of this multi-storey frame can be expressed in terms of the rotation $\theta(s)$ in the whole loaded column

$$\begin{cases} u = \int_0^h \sin \theta(s) ds \\ v = h - \int_0^h \cos \theta(s) ds \end{cases} \quad (69)$$

The virtual displacement field considered in the kinematic approach is the rigid mechanism defined by (see Fig. 12)

$$\delta\theta(s) = \delta\theta_0 \text{ for } s \in [0; h_0] \text{ in the two columns; } \delta\theta(s) = 0 \text{ otherwise} \quad (70)$$

h_0 is the height of the first floor. This is typically a shear virtual mechanism. In this case, Eq. (45) is expressed by

$$H\delta\theta_0 \int_0^{h_0} \cos \theta(s) ds + P\delta\theta_0 \int_0^{h_0} \sin \theta(s) ds \leq 2M_p |\delta\theta_0| \quad (71)$$

which leads to the following inequality

$$-2M_p \leq H(h_0 - v_0) + Pu_0 \leq 2M_p \quad (72)$$

u_0 is the horizontal displacement of the first floor point connected to the loaded column and v_0 is the vertical displacement of the same point. In this case, the kinematics bound does not depend on the displacement of the loaded points.

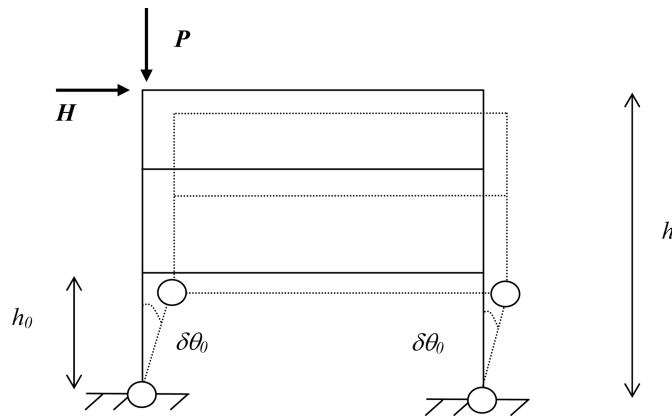


Fig. 12 Multi-storey single-bay portal – shear mechanism

10. Conclusions

The kinematical approach of limit analysis has been rigorously applied to frame structures, taking into account the geometrical changes of the structures. In the most general case, the kinematic approach leads to an upper bound which is a functional of the true unknown displacement functions (obtained by solving the elastoplastic evolution problem). For the so-called exact geometry analysis, the results are generally difficult to use (see for instance Eq. (63)), except for simple mechanisms. The theoretical bound is more easily readable assuming small rotations, also-called second-order analysis theory. The reasoning and the results are different from those of the original method developed in the sixties, based on the coincidence of the virtual displacement field with the true mode of collapse (Onat 1955, Massonnet and Save 1961, Horne 1963). An admissible load-displacement plane is then defined, according to the theory of yield design (Salençon 1992). It has been shown that the displacement involved in this bound could differ from that of the point of the applied limit load. The theoretical function is an upper bound of the true load-displacement function obtained during the monotone elastoplastic evolution. This function can be used for instance in the optimal design of steel frames in seismic area. Finally, extension of the present results to inextensible plates or shells could be also theoretically investigated, although the kinematics in such a case is naturally more complex (see the recent paper of Farmer and Calladine 2005).

The geometrical analysis proposed in this paper is based on the strong assumption that beam members are not extensible. This restriction can be discussed. In fact, the kinematical variables of the problem may be chosen as the axial strain of the middle fibre ε , and the curvature χ , whose dual static associated variables are the normal force N and the bending moment M . Although it has been assumed that strength members only depend on the moment variables, strength criterion generally depends on the two static variables (N, M) . This interaction diagram can play a significant role as shown by Siemaszko and König (1982), even in small displacement analysis. This influence is quite difficult to show analytically, while general existing mechanisms only consider hinge mechanisms, without any axial displacement discontinuities. Numerical results, based on second-order analysis, or on the so-called geometrically exact analysis are then required to enrich the applied engineering results obtained in this paper.

References

- Antman, S.S. (1995), *Nonlinear Problems of Elasticity*, Springer-Verlag, New-York.
- Arakélian, V. (1997), *Structure et cinématique des mécanismes*, Hermès, Paris (in French).
- Bazant, Z.P. and Cedolin, L. (2003), *Stability of Structures: Elastic, Inelastic, Fracture and Damage Theories*, Dover Publications, New-York.
- Bernal, D. (1987), "Amplification factors for inelastic dynamic p-delta effects in earthquake analysis", *Earthq. Eng. Struct. Dyn.*, **15**, 635-651.
- Calladine, C.R. (1968), *Simple Ideas in the Large-deflection Plastic Theory of Plates and Slabs*, in: Heyman, J., Leckie, F.A., editors, *Engineering Plasticity*, Cambridge University Press, 93-127.
- Chakrabarty, J. (2007), *Applied Plasticity*, Mechanical Engineering Series, Springer.
- Challamel, N. (2006), "Large displacement limit analysis of frame structures", *Stability and Ductility of Steel Structures*, D. Camotim *et al.* (Eds), Lisbon, Portugal, September 6-8, 2006.
- Challamel, N. and Pijaudier-Cabot, G. (2006), "Stability and dynamics of a plastic softening oscillator", *Int. J. Solids Struct.*, **43**, 5867-5885.
- Chan, S.L. and Zhou, Z.H. (2004), "Elastoplastic and large deflection analysis of steel frames by one element per

- member II: Three hinges along member”, *J. Struct. Eng.*, **130**(4), 545-553.
- Chiou, Y.J., Wang, Y.K., Hsiao, P.A. and Chen, Y.L. (2002), “Large displacement analysis of inelastic frame structures by convected material frame approach”, *Struct. Eng. Mech.*, **13**(2), February.
- Climenhaga, J.J. and Johnson, P.P. (1972), “Moment-rotation curves for locally buckling beams”, *J. Struct. Div.* **98**, 1239-1254.
- De Freitas, J.A.T. and Smith, D.L. (1984), “Existence, uniqueness and stability of elastoplastic solutions in the presence of large displacements”, *Solid Mech. Arch.*, **9**, 433-450.
- Duszek, M.K. and Lodygowski, T. (1983), *On Influence of Some Second Order Effects on the Post-yield Behaviour of Plastic Structures*, in: Sawczuk, A., Bianchi, G., editors, *Plasticity today – Modelling, Methods and Applications*, Elsevier Applied Science Publishers, 413-428.
- Elnashai, A.S. (2001), “Advanced inelastic static (pushover) analysis for earthquake applications”, *Struct. Eng. Mech.*, **12**(1), July.
- Farmer, S.M. and Calladine, C.R. (2005), “Geometry of “developable cones”, *Int. J. Mech. Sci.*, **47**, 509-520.
- Feng, L. and Tong-Xi, Y. (1991), “An analysis of the large deflection of an elastic-plastic cantilever subjected to an inclined concentrated force”, *Appl. Math. Mech.*, **12**(6), 547-555.
- Gürkök, A. and Hopkins, H.G. (1973), “The effect of geometry changes on the load carrying capacity of beams under transverse load”, *SIAM J. Appl. Math.*, **25**(3), 500-521.
- Horne, M.R. (1963), “Elastic-plastic failure loads of plane frames”, *Proc. Roy. Soc. London, Serie A*, **274**, 343-364.
- Horne, M.R. and Merchant, W. (1965), *The Stability of Frames*, Pergamon Press, Oxford.
- Horne, M.R. (1995), *The Rankine-Merchant Load and Its Application*, In *Summation Theorems in Structural Stability*, Ed. T. Tarnai, 111-139 (CISM Courses and Lectures No. 354. Springer-Verlag, Wien, New York).
- Jennings, P.C. and Husid, R. (1968), “Collapse of yielding structures under earthquakes”, *J. Eng. Mech. Div.*, ASCE, **94**, 1045-1065.
- Jirasek, M. and Bazant, Z.P. (2002), *Inelastic Analysis of Structures*, Wiley, New-York.
- Lance, R.H. and Soechting, J.F. (1970), “A displacement bounding principle in finite plasticity”, *Int. J. Solids Struct.*, **6**, 1103-1118.
- Leu, L.J. and Tsou, C.H. (2001), “Second order analysis of planar steel frames considering the effect of spread of plasticity”, *Struct. Eng. Mech.*, **11**(4), 423-442.
- Liew, R.J.Y., White, D.W. and Chen, W.F. (1993), “Second-order refined plastic-hinge analysis for frame design”, *J. Struct. Eng.*, **119**(11), 3196-3216.
- Maier, G. and Drucker, D.C. (1973), “Effects of geometry changes on essential features of inelastic behaviour”, *J. Eng. Mech. Div.*, ASCE, **99**, 819-834.
- Massonnet, C. and Save, M. (1961), *Calcul plastique des constructions*, Centre Belgo-Luxembourgeois d’information de l’acier, Bruxelles (in French).
- Mazzolani, F.M. and Gioncu, V. (2002), *Ductility of Seismic-resistant Steel Structures*, Spon Press, London.
- Merchant, W. (1954), “The failure load of rigid jointed frameworks as influenced by stability”, *Struct. Eng.*, **32**, 185-190.
- Onat, E.T. (1955), “On certain second-order effects in the limit design of frames”, *J. Aeronaut. Sci.*, **22**, 681-684.
- Polizzotto, C. and Borino, G. (1996), “Shakedown and steady-state response of elastic-plastic solids in large displacements”, *Int. J. Solids Struct.*, **33**, 3415-3437.
- Salençon, J. (1966), “Expansion quasi-statique d’une cavité dans un milieu élastoplastique”, *Annales des Ponts et Chaussées*, **3**, 175-187 (in French).
- Salençon, J. (1990), “An introduction to the yield design theory and its application to soil mechanics”, *Eur. J. Mech A/Solids*, **9**(5), 477-500.
- Salençon, J. (2002), *De l’élastoplasticité au calcul à la rupture*, Editions de l’Ecole Polytechnique, Ellipses, Paris, 2002 (in French).
- Save, M.A., Massonnet, C.E. and de Saxce, G. (1997), *Plastic Limit Analysis of Plates, Shells and Disks*, North-Holland Series in Applied Mathematics and Mechanics, Elsevier, Amsterdam.
- Shanmugan, N.E. and Wang, C.M. (2005), *Analysis and Design of Plated Structures (Volume 1: Stability)*, Woodhead Publishing Limited.
- Siemaszko, A. and König, J.A. (1982), “Analysis of stability of incremental collapse of skeletal structures”, *J.*

- Struct. Mech.*, **13**, 301-312.
- Wang, B., Lu, G and Yu, T.X. (1995), "A numerical analysis of the large deflection of an elastoplastic cantilever", *Struct. Eng. Mech.*, **3**(2), March.
- Weichert, D. (1990), "Unified formulation of statical shakedown criteria for geometrically nonlinear problems", *Int. J. Plast.*, **6**, 433-447.
- Yang, Y.B., Yau, J.D. and Leu, L.J. (2003), "Recent developments in geometrically nonlinear and postbuckling analysis of framed structures", *Appl. Mech. Rev.*, **56**(4), 431-449.
- Yu, T.X. and Johnson, W. (1982), "The plastica: The large elastic-plastic deflection of a strut", *Int. J. Non-linear Mech.*, **17**, 195-209.
- Yu, T.X. and Zhang, L.C. (1996), *Plastic Bending – Theory and Applications*, Series on Engineering Mechanics, Vol. 2, World Scientific, Singapore.
- Zhou, Z.H. and Chan, S.L. (2004), "Elastoplastic and large deflection analysis of steel frames by one element per member I: One hinge along member", *J. Struct. Eng.* **130**(4), 538-544.
- Ziegler, H. (1968), *Principles of Structural Stability*, Blaisdell Publishing Company, London.